Berm Breakwater Design

Influence of Movements on Stone Durability

Hald, Tue; Frigaard, Peter; Burcharth, H. F.; Sigurdarson, S.

Published in:
Proceedings of the Final Workshop Berm Breakwater Structures, Iceland, Nov. 1996

Publication date:
1996

Document Version
Early version, also known as pre-print

[Link to publication from Aalborg University](#)

Citation for published version (APA):
Hald, T., Frigaard, P., Burcharth, H. F., & Sigurdarson, S. (1996). Berm Breakwater Design: Influence of Movements on Stone Durability. In *Proceedings of the Final Workshop Berm Breakwater Structures, Iceland, Nov. 1996*

BERM BREAKWATER STRUCTURES
MAS2 – CT94 –0087

Berm Breakwater Design

Influence of Movements on Stone Durability

November 1, 1996

Berm Breakwater Design
Influence of Movements on Stone Durability

T. Hald, P. Frigaard, H.F. Burcharth, Hydraulics & Coastal Engineering Laboratory, Aalborg University, Sohngaardsholmsvej 57, DK-9000 Aalborg, Denmark, fax +45 98142555

Sigurdur Sigurdarson, Icelandic Harbour Authority, Vesturvor, 2200 Kopavogur, Iceland

1   Introduction

Traditionally, conventional rubble mound breakwaters are designed with stable armour units, and consequently, very large stones or even artificial armour units are required. Reshaping breakwater designs allow reshaping of the seward slope thus involving stone movements. Ultimately, dependent on the degree of safety in the design, this reshaping process might end up in a stable profile where no changes in the cross sections occur even though stone movements are allowed.

Unfortunately, large movements of the protecting stones during the structural lifetime in combination with high stone velocities inherently causes some breakage and abrasion of the individual stones and thereby also reduced stability. In order to avoid excessive abrasion a high stone quality is demanded or larger stones must be applied when constructed. To allow the designer to account for abrasion and armour stone breakage due to the stone motion a description of the overall wave climate during the structural lifetime must be derived involving knowledge of transport rates, movement patterns, stone velocities and stone quality.

The main objective of the paper is to describe a tool enabling calculation of the anticipated armour stone movements. Also tensile stresses occur, as a result of stone against stone impact are discussed in order to make a more close connection between wave climate, stone movements and abrasion/breakage. Finally, a comparison to selected prototype structures is made to compare the armour stone movement model with visual profile observations of exciting breakwaters.

2   Longshore Transport Rate

Motion of stones along the active profile occurs when even slightly oblique waves attack the breakwater. This longshore motion have been evaluated in model tests performed by Burcharth and Frigaard (1988) and by van der Meer and Veldman (1992). Longshore transport was measured by observing the movements of stones layed out in coloured bands over the profile. To calculate the steady state transport the number of stones per wave passing a specific cross section at each sea state was divided by the number of waves. This ratio is termed the longshore transport rate S_x.

In figure 1 the measured longshore transport rate is plotted against the mobility index $H_o T_{op} = \frac{H_s}{\Delta D_{n50}} \, T_p \sqrt{\frac{g}{D_{n50}}}$. The longshore transport rate seems to be described quite well by the power function originally proposed by Vrijling (1991)

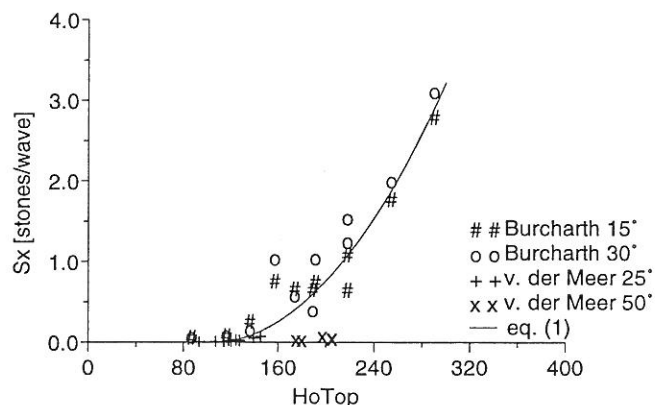$$S_x = 85 \cdot 10^{-6}(H_o T_{op} - 105)^2 \qquad (1)$$

Figure 1: Longshore transport rate for reshaping breakwaters.

One might argue if the model in eq. (1) is too simple because of the absence of obliqity. The model can however, easily be adjusted to include the angle of incidence θ as discussed by Alikhani et al. (1996).

Another aspect of the transport model is the obvious sensitivity to the onset of motion. From the model it is seen that sea states slightly above those corresponding to the onset of motion result in significant transport due the rapid increase of the power function. The latter comparison with prototype breakwaters outline this sensitivity.

3 Longshore Distribution of Transported Material

To characterize the motion of the individual stones on the breakwater several video recordings from the model tests performed by Burcharth and Frigaard (1988) have been analysed thoroughly.

The main conclusion based on the analysis of the video recordings was a typical zigzag motion pattern as shown in figure 2. The typical upward motion of the stone follows the wave direction
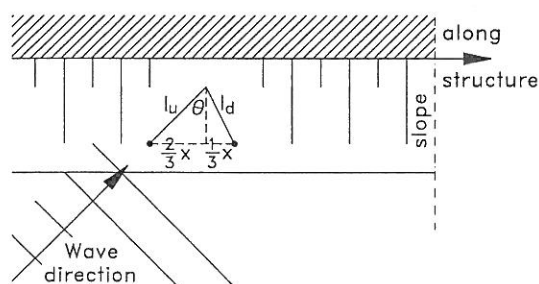

Figure 2: Typical pattern for single stone motion.

θ whereas the downward motion is more controlled by gravity and an angle of half the angle of incidence seems more appropiate, see figure 2. From figure 2 the total travelled longshore distance can be calculated, assuming the upward and downward distances orthogonal to the structure in average are equal

$$l = l_u + l_d = \frac{2x}{3\sin(\theta)} + \frac{x}{3\sin(\frac{1}{2}\theta)} \qquad (2)$$

To quantify the travelled longshore distance x the longshore distribution of the transported material has been derived from the same tests. The longshore distribution was derived from recordings of the number of stones positioned in 5 cm wide bands over the profile along the entire length of breakwater. From these recordings the number of stones per m, the position of the individual stones and the mean stone movements are calculated. Figure 3 shows an example from a single longshore transport test.

Figure 3: Example of the longshore distribution of transported material.

In figure 4 the longshore distribution is shown for all 22 tested wave climates. As abscissa the travelled longshore distance x is normalized by the mean travelled distance $\bar{x}$ and as ordinate the stone distribution along the structure $s(x)$ (unit: stones/m per wave) is normalized by multiplying with $\frac{\bar{x}}{S_x}$. From figure 4 an excellent uniformity of the distribution curves for different wave climates and different angles of incidence is seen. Hence, a general exponential function can be fitted to the entire data set

$$s(x) = 0.6\exp(-0.6\frac{x}{\bar{x}})\frac{S_x}{\bar{x}} \qquad (3)$$

In figure 5 the mean stone movement is plotted against the mobolity index for all 22 tested wave climates. The mean stone movement is described by

$$\bar{x} = 4.3 \cdot 10^{-3} D_{n50}(H_o T_{op} - 105)\sin^{0.8}(2\theta) \qquad (4)$$

or by inserting the longshore transport model eq. (1).

$$\bar{x} = 0.5 D_{n50}\sqrt{S_x}\sin^{0.8}(2\theta) \qquad (5)$$

Inserting the mean travelled distance in the expression for l, eq. (3) gives the average distance moved per wave. Knowing the wave height/period scatter diagram describing the storm history
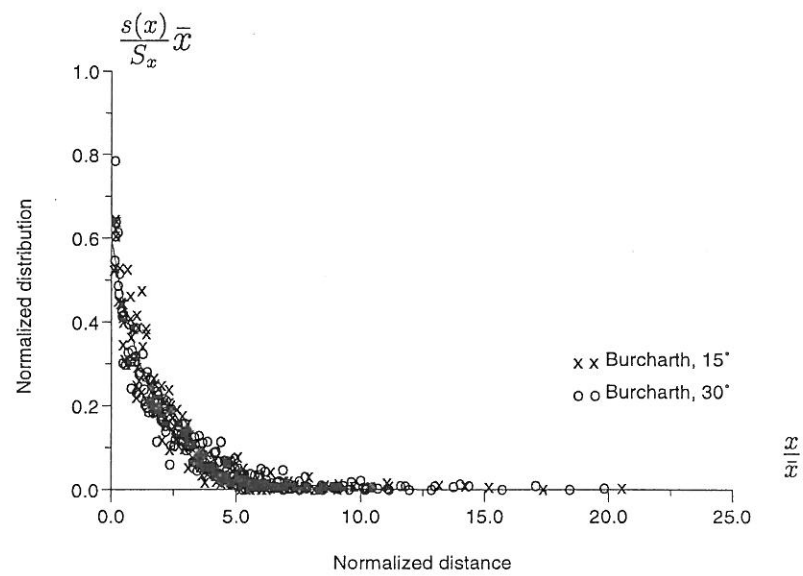
$$\frac{s(x)}{S_x}\bar{x}$$

Figure 4: Longshore distribution of transported material.

Figure 5: Mean stone movement versus the mobility index.

for a specific area, it is possible to calculate the accumulated average distance moved by each single storm during the structural lifetime simply based on the easy accessible parameters, H_s, T_p, θ, number of waves and D_{n50}.

4   Impact Stresses in Armour Stones

A more close description than the stone motion connecting abrasion and breakage is to consider the tension stresses as a result of armour stones impacting armour stones during movements. This impact results in a shock wave propagating through the stone which is reflected at the edge structure resulting in a reverse propagating tensile stress wave. In case the tensile stress is too high the stone may crack depending on the stone quality.

In figure 6 an idealized static model of a stone impact is sketched where the impacted stone remains at rest after impact. This is modelled by giving the stone infinity mass and zero velocity.

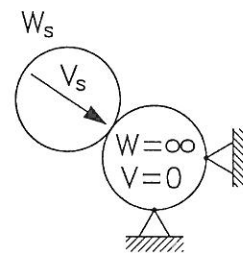Applying Hertz' law to the system in figure 6 results in the following equation

Figure 6: Static model

$$\sigma_{max} \propto \left(\frac{V_s^4}{D_{n50}} \right)^{0.2} E \qquad (6)$$

where:

W_s	= Stone weight
V_s	= Stone velocity
D_{n50}	= Nominal stone diameter
E	= Young's Modulus

Generally, eq. (6) describes the stresses with reason: a high velocity yields high stresses, a small diameter signifies large curvature and thus larger impact stresses because of the smaller contact area, and finally the elasticity of the stone is described by Young's Modulus. Another aspect is that by simple Froude scaling larger stones gain larger stresses.

From the previously described tests typical stone velocities during both run-up and run-down were investigated by video. A typical stone velocity during run-down equals the wave run-down velocity whereas the typical stone velocity during run-up is approximately 50-70% of the wave run-up velocity.

Several attempts to assess the run-up and run-down velocities have been made showing that the maximum expected velocity can be well described by H_s and $\xi = g(\alpha, H_s, T_p)$. The overall maximum velocity is expected to be in the order of $1.5\sqrt{gH_s}$, e.g. Bruun, (1979).

From the above considerations it seems that the impact stresses can be described by the same easy accessible parameters as the movement model. The model still needs verification and calibration to physical model tests as well as prototype measurements. More work has to be done into these subjects.

5 Comparison with Protoype Breakwaters

For prototype comparison four sites are investigated with wave and structural characteristics given in the following two tables. The accumulated travelled mean distance have been calculated followingly:

- Calculation of longshore transport rate from eq. (1) for each storm.

- Calculation of mean position moved from eq. (5) for each storm.

- Calculation of total travelled distance from eq. (3) for each storm.

- Summation of total travelled distance during lifetime.

Regarding

1. Caldera, Costa Rica: Estimated stone movements are rather small indicating little stone movements during lifetime. Observations shows little profile changes but some broken stones due to the very poor quality of the stones.

2. St. Pauls, Alaska: Very large stone movements are estimated. Total damage of the brakwater was observed.

3. Racine, Wisconsin: Long travelled distance is estimated. Severe breakage and large profile changes were observed.

4. Bolungarvik, Iceland: Little stone motions were estimated. Little profile changes observed.

It seems that the calculated distance corresponds very well to what might have happend. Though, it is clear that actual damage depends on both the travelled distance and the quality of the stones. I all, the comparison indicate that there is reason in relating breakwater damage to the armour stone motion.

Location	W_{50} [t]	ρ [t/m³]	storm	duration [waves]	H_s [m]	T_p [sec]	Θ [deg]	H_0	$H_0 T_{0p}$	S [stones/wave]	l_i [m]
Caldera, Costa Rica	5.0	2.40	21.09.78	3000	3.65	18.7	50	2.1	109.5	$1.7 \cdot 10^{-3}$	129
	5.0	2.40	21.05.81	3000	3.55	17.9	50	2.1	101.2	0	0
	5.0	2.40	18.07.83	3000	3.47	17.1	50	2.0	95.2	0	0
	5.0	2.40	18.06.78	3000	3.30	17.5	50	1.9	92.6	0	0
St. Pauls, Alaska	1.5	2.77	13.11.84	1900	5.34	31.0	15	3.8	417.1	8.3	6572
	1.5	2.77	07.12.84	4000	5.34	15.0	15	3.8	201.8	0.8	4296
Racine, Wisconsin	0.82	2.61	08.03.87	2500	4.4	11.2	15	4.15	176.6	0.4	1653
Bolungarvik, Iceland	6.0	2.85	27.10.95	3000	6.0	15	10	2.65	109.9	$2.0 \cdot 10^{-3}$	282

Location	Stone type/ shape	W_{50} [t]	ρ [t/m³]	$\frac{W_{85}}{W_{15}}$	$H_{0,max}$	$H_0 T_{0p,max}$	S_{max} [stones/wave]	$\sum l_i$ [m]	Visual profile observations
Caldera, Costa Rica	Sand stone/ Rough angluar	5.0	2.40	1.5	2.1	110	$1.7\ 10^{-3}$	129	app. 5-10% broken stones, severe abrasion, little profile changes and longshore transport
St. Pauls, Alaska	Crushed stone	1.5	2.77	3.0	3.8	417.1	8.3	10868	total damage, 150 m recession of breakwater head
Racine, Wisconsin	Crushed limestone	0.82	2.61	2.5	4.15	176.6	0.4	1653	severe breakage of armour stones, large profile changes and longshore transport
Bolungarvik, Iceland	Quarry stone/ Rough angular	6.0	2.85	2.5	2.65	109.9	$2.0\ 10^{-3}$	282	no armour stone breakage, little profile changes, no longshore transport

6 Conclusions

A model enabling calculation of the accumulated travelled stone distance is given based on the easy accessible parameters such as H_s, T_p, θ, number of waves and D_{n50}. Furthermore, a short discussion focussing on the stuctural integrety is given. It is argumented that the anticipated maximum tensile impact stresses can be evaluated by the same easy accessible parameters, though more work need to be done into this subject.

A comparison with selected prototype structures is presented showing that there is reason in relating breakwater damage to the armour stone motion. The comparison also signifies that only little transport should be allowed in order to avoid severe damage.

7 References

Alikhani, A., Tomasicchio, R. and Juhl, J., *Berm Breakwater Trunk Exposed to Oblique Waves*, to be published in Proc. 25th ICCE, Orlando, USA, 1996.

Burcharth, H.F., Frigaard, P., *On 3-Dimensional Stability of Reshaping Breakwaters*, Proc. 21th ICCE, Malaga, Spain, 1988.

Bruun, 1979

CIRIA/CUR, *Manual on the Use of Rock in Coastal and Shoreline Engineering*, Published jointly by the Construction Industry Research and Information Association in the UK and the Centre for Civil Engineering Research, Codes and Specifications in the Netherlands, 1991.

Lamberti, A., Tomasicchio, G.R., *Stone Mobility and Abrasion on Reshaping Breakwaters* to be published in Coastal Engineering, 1996.

Van der Meer, J.W., Veldman, J., *Singular Points at Berm Breakwaters: Scale Effects, Rear, Round Head and Longshore Transport*, Coastal Engineering, Vol. 17, Nos. 3,4, August 1992.

Vrijling, J.K., Smit, E.S.P. and Swart, P.F., *Berm Breakwater Design; the Longshore Transport Case: a Probabilistic Approach*, ICE, Proc. Coastal Structures and Breakwaters, London, 1991.

Sigurdarson, S., Viggosson, G., *Berm Breakwaters in Iceland, Practical Experiences*, Proc. Int. Conf. on Hydro-Technical Engineering for Port and Harbour Construction, Yokosuka, Japan, October 1994.

$$\frac{\overline{X}}{\alpha_L \sin^{0.8} 2\Phi}$$

total variance

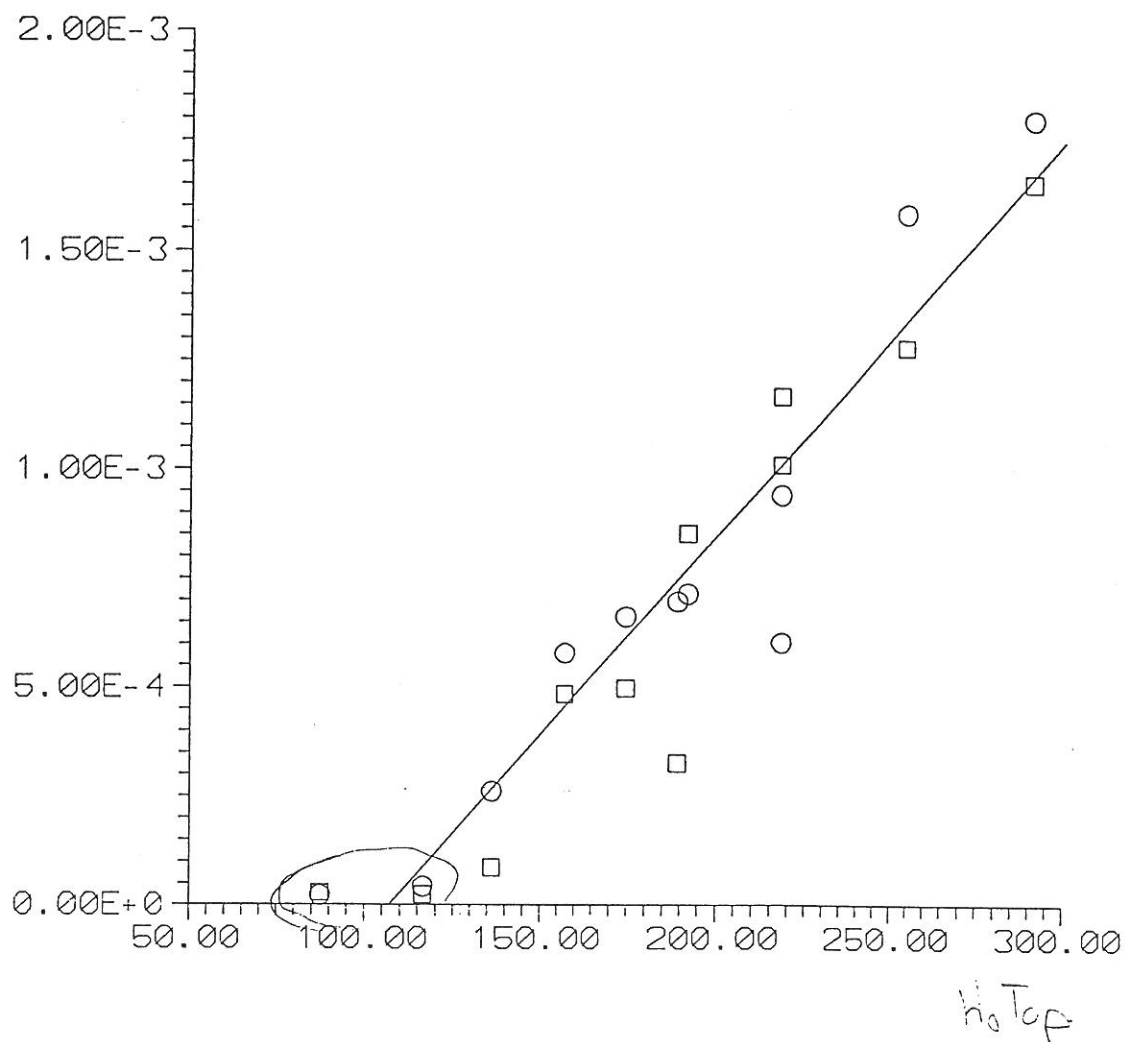$$\overline{X}_{total} = \alpha_L \overline{X}'$$

$$\alpha_L \approx 2.6$$

$h_0 T_{0F}$

Figure 5